# A New Approach to Improve Film Cooling Effectiveness Using Combined Jets

A. Javadi[1, 2], K. Javadi[1,3], M. Taeibi-Rahni[3], and M. Darbandi[3]

[1]Aerospace Research Institute (ARI) – Ministry of Science, Research and Technology – Tehran P.O. Box 15875-3885, Iran.
Tel: 098-21 8362010, Fax: 098-21 8362011, E-mail: javadi_ali@ari.ac.ir
Departments of Chemical Engineering[2] and Aerospace Engineering[3],
Sharif University of Technology (SUT) Tehran P.O. Box 11365-9465, Iran
Tel: 098-21 600 5819, Fax: 098-21 602 2853, E-mail: javadi@mehr.sharif.edu

## Abstract

To achieve a high film cooling effectiveness in gas turbine blades, most investigations are concentrated on the effects of the holes shape, jet angle, blowing ratio, jets arrangement, coolant temperature, etc. This research develops a new scheme to achieve this purpose by the control the wake zones behind the coolant jet and reduction of mixing strength, between the two hot (main Stream) and cold streams (coolant jets), using combined jets. The primitive idea originates from our previous research on jet-to-crossflow [Javadi et al. (2002)] where the significant role of mixing zones in destroying the coolant film was obviously observed. In that research, we computationally simulated a three-dimensional, separated holes film cooling problem of flow over a flat plate (ordinary film cooling system), using Reynolds stress turbulence model (RSM). The comparison of our results with the experimental data [Ajersch et al. (1995)] showed that, the RSM/SST turbulence model in our work has better agreement with experimental data in most cases. In this research, we have considered a new combined jets system including main coolant jet and two additional coolant small jets (coupled), downstream of the main jet in order to control the interaction and mixing between two hot and cold streams. Note, in order for the results to be comparable, total coolant air and the cross section area of the new combined jets system are the same as the previously used single jet (ordinary system). The results show a significant enhancement in film cooling effectiveness in addition to a good improvement in uniformity of the coolant film on the plate. For better understanding of the mechanism of this improvement, the role of the new weak wakes generated by the coupled jets beside the strong main wakes generated by main jet is discussed. These new weak wakes reduce the interaction and mixing process the hot and main cooled stream like a fluid barrier while they do not have themselves high interactions with hot stream. On the other hand it seems that not only the interaction between the new weak wakes and the main strong wakes isn't undesirable, but also it is useful for accomplishing a desirable momentum and energy transport in spanwise direction and achieves a uniform coolant film. Hence, the improvement of the cooling uniformity is another benefit of this new scheme, which will be the subject of our future work.

**Keywords:** Film Cooling, Gas Turbine Blades, Turbulence Modeling, Crossflow.

## Nomenclature

| | |
|---|---|
| $a$ | Speed of Sound |
| $C_1', C_2', C_\mu$ | Empirical Constants in RSM Model |
| $C_1'\ C_2, C_{1,} C_s$ | Empirical Constants in RSM Model |
| $C_{ij}$ | Convection Term in RSM Model |
| $D_{ij}$ | Jet Diameter |
| $d$ | Normal Distance to the Wall (Eq. 12 ) |
| $D_{ij}^L$ | Molecular Diffusion in RSM Model |
| $D_{ij}^T$ | Turbulent Diffusion in RSM Model |
| $F_1, F_2$ | Switching Function in ($\kappa - \omega$) Model |
| $F_{ij}$ | Production by System Rotation |
| $G_{ij}$ | Buoyancy Production |
| J | Momentum Ratio $J = (\rho_{jet} V_{jet}^2) / \rho_{cf} V_{cf}^2$ |
| $k$ | Turbulence Kinetic Energy |
| $M_t$ | Mach Number |
| $P_{ij}$ | Stress Production in RSM Model |
| $R = V_{jet} / V_{cf}$ | Jet-to-Cross Flow Velocity Ratios |
| $\overline{U}, \overline{V}, \overline{W}$ | Mean Velocity Components |
| $\overline{U_i}$ | Mean Velocity Components |
| $U_i$ | Instantaneous Velocity Components |
| $u_i$ | Fluctuation Velocity Components |
| $\overline{u_i u_j}$ | Reynolds Stresses |
| $\eta_k\ \ x_k$ | Component of the Unit Normal to the Wall |
| $\mu$ | Viscosity |
| $\sigma_k, \sigma_\omega, \sigma_{\omega 2},$ | Empirical Constants in SST Model |
| $\beta, \beta^*, \gamma$ | Empirical Constants in SST Model |
| $\sigma_k$ | Prandtl Number |
| $\rho$ | Density |
| $\phi$ | Dependent Variable Except V (Eq. 20) |
| $\phi_{ij}$ | Pressure Strain Terms in RSM Model |
| $\phi_{ij,1}$ | Slow Pressure-Strain in RSM Model |
| $\phi_{ij,2}$ | Rapid Pressure-Strain Term |
| $\phi_{ij,3}^\omega$ | Wall-Reflection Term in RSM Model |
| $\varepsilon$ | Turbulence Energy Dissipation Rate |
| $\varepsilon_{ij}$ | Dissipation Tensor |
| $\omega$ | Specific Dissipation Rate $(\varepsilon / \beta^* k)$ |
| $\mu_t$ | Eddy Kinematics viscosity |
| $\tau_{ij}$ | Reynolds Stresses |

**INTRODUCTION AND LITERATURE REVIEW**

Improvement the efficiency of the thermodynamic cycles in the power plants and propulsion engines can be achieved through higher gas turbine entry temperature. However high inlet temperatures those are sufficient to damage the blades requires the development of material and efficient cooling methods. Various methods for cooling of different parts of aircraft propulsion systems have been investigated for more than 50 years. Comparison of the effectiveness of convection, transpiration, and film cooling methods with air as coolant is one of the oldest investigations by Eckert and Livingood (1954). In their analytical/numerical investigation, film cooling was studied as a new method for cooling of gas turbine engine components. Next investigations showed that film cooling is one of the best methods that have gained increasing importance.

In film cooling process, the secondary coolant airflow is bypassed from the compressor and is ejected through the blade surface into the external boundary layer in order to reduce the temperature in the boundary layer and to protect the surface over which the hot gas flows. Due to manufacturing and stress-related reasons, hole injection film cooling is preferred rather than slot injection film cooling. The discrete-hole geometry leads to a three-dimensional flow .The intensive cooling of blades and vanes in modern gas turbines is required to guarantee an economically acceptable life span of the components, which are in contact with the hot gas. For this aim, we need to understand the complex cross flow in more detail. Although film cooling phenomenon have been investigated for several years, basic investigations are still necessary to understand the complex mixing and secondary flow characteristics, some investigation in this field are reviewed in below.

Amer et al. (1992) used different turbulence models to predict film cooling from two rows of holes inclined in the streamwise direction. Their models were the $\kappa-\omega$ model and its modified version, as well as the standard $\kappa-\varepsilon$ model, together with its non-isotropic version. Comparison between the predicted results using these models and the previous experimental data indicated that the ability of a turbulence model to predict the experimental results depends strongly on the blowing ratio as well as on the distance downstream from the injection holes. Also, they investigated the effects of the various coolant velocities of the injection holes for the prediction of film cooling.

Kim and Benson (1993) calculated a three-dimensional turbulent flow of a jet in a cross-flow using a multiple-timescale turbulence model. Their computational domain included a circular jet channel such that the interaction between the jet and the cross-flow could be simulated more accurately. Their work showed that the row of jets in a cross-flow is characterized by a highly complex flow-field, including a horse shoe vortex and two helical vortices.

Ajersch et al. (1995) have also studied the flow of a row of six square jets injected at 90 degrees to a cross flow, both experimentally (using a three-component Laser Doppler velocimeter) and computationally. Their jet-to-cross flow velocity ratios examined were 0.5, 1.0, and 1.5 and their jet Reynolds number was 4700. Also, the spacing-to-jet-width ratio was 3.0. They measured the mean velocities and six Reynolds stresses using a three component LDV operating in coincidence mode. Their numerical simulation of the flow was performed using a multi grid, segmented, k-$\varepsilon$ , computational fluid dynamics code.

Hassan et al. (1998) numerically investigated the flow-field of a single row of compound-angle jets in a cross flow, using different zonal $(\kappa-\varepsilon)/(\kappa-\omega)$ turbulence models. Their results were compared with previous experimental data for jet-to-cross-flow velocity ratios of 0.5 and 1.5. These comparisons indicated that the ability of the zonal $(\kappa-\varepsilon) / (\kappa-\omega)$ turbulence models to predict the flow-field of a jet in a cross flow depends strongly on the velocity ratio as well as on the distance downstream from the injection holes.

Keimasi and Taeibi-Rahani (2001) also computationally simulated a three-dimensional and incompressible flow-field of square jets injected perpendicularly into a cross-flow over a flat plate. Their jet-to-cross flow velocity ratios were 0.5, 1.0, and 1.5, also their jet Reynolds number was 4700. Also, their spacing-to-jet-width ratio in one row of holes was 3.0. They solved the Reynolds averaged Navier-Stocks (RANS) equations (including the energy equation) in the general form, using the SIMPLE finite volume method over a non-uniform staggered grid. For the turbulence modeling, they used standard k-$\varepsilon$ model with wall functions and zonal $(\kappa-\varepsilon) / (\kappa-\omega)$ turbulence model (shear stress transport model or SST). The results of the two different turbulence models were compared with the Ajersch et al. (1995) experimental data. Their results indicated that, the ability of the SST model to predict the film cooling flow-field depends strongly on the velocity ratio as well as on the distance downstream of the jet. Their computational results showed better agreements with experimental data (especially the mean streamwise velocity profiles).

Javadi et al. (2002) also computationally simulated a three-dimensional and incompressible flow-field of square jets injected perpendicularly into a cross-flow over a flat plate in a system same as Keimasi and Taeibi (2001) but using RSM/SST turbulence modeling. The jet-to-cross flow velocity ratios, $R = Vjet / Vcf$ , (blowing ratios) were selected to be 0.5 and 1.5, and the jet Reynolds number was 4700 in wich the subscript jet corresponds to the jet flow and the subscript cf corresponds to the cross flow. The flow-field at the jet exit was three-dimensional and strongly depends on the jet-to-cross flow velocity ratios. Thus, the flow in the jet channel was solved together with the flow over the flat plate. Results was compared with Ajersch et.al. (experimental LDV and numerical work's, $\kappa-\varepsilon$ turbulence model) and Keimasi and Taeibi-Rahani's numerical simulation work (SST turbulence model). Comparison between the measured and computed results showed, that RSM/SST turbulence model in their work has better agreement with experimental data in most cases. In this research in order to control of mixing process between two hot and cooled streams we have designed coupled jets beside the main jet. The base of this idea came from our previous researches on jet-to-crossflow film cooling in which we understood the significant effect of mixing zones on ruin of coolant film. The new system has been designed with a same coolant air and total cross section of coolant holes relative to previously system. In the other hand summation of coolant rate and cross section of two coolant small holes (coupled jets) and main jet in new system is equal to previous hole. Our results show a significant enhancement in film cooling effectiveness with a good improvement of uniformity of the coolant film on the plate. For better understanding of the

mechanism of this improvement, the role of the new weak wakes generated by coupled jets beside the strong main wakes generated by main jet is discussed. These New weak wakes like a fluid barrier reduce the interaction and mixing process of the hot and main cooled stream while they themselves do not have a high interaction with hot steam. In the other hand it seems that not only the interaction between the new weak wakes and main strong wakes isn't undesirable, but also is useful for accomplishing a desirable momentum and energy transport in span wise and achieving a uniform coolant film. Hence the improvement of cooling uniformity is another benefit of this new scheme which will be the subject of our next paper. Also investigation of capability of using suction stream instead of blowing in coupled jets, hole shape, jet angle, blowing ratio, jets array, and coolant temperature effects in this new scheme are our current or future works.

**TURBULENT FLOW GOVERNING EQUATIONS**

At present in absent of exact solution and for access a good flow field parametric study, computational solutions of full Navier-Stokes equations for 3-D complex flow, are a desirable way and very economic for decrease of high expensive and difficult experimental study for understanding of engineering processes. Direct numerical simulation (DNS), Reynolds-averaged Navier-Stokes (RANS), and large eddy simulation are three various approach for this purpose. DNS approach needs a very fine computational grid that causes a high computational cost with an unacceptable time. LES approaches although seem hopefulness in future, currently need more experience and also they need a fine computational grid yet due to existing DNS approach in theirs sub-domain.

In the other hand the correct prediction of film-cooling and associated heat transfer is directly related to the prediction of jet-to-crossflow mixing, which represents the major difficulty. The majority of turbulence models fail for this flow configuration. Because of the presence of multiscale flow phenomena, more fundamental approaches such as LES or DNS are computationally impractical (Medic G. and Durbin P. 2001). However, it seems that RSM/SST turbulence models have the potential of greater accuracy and wider applicability for prediction of cross-flow jet mixing in film cooling problems. They are usually very successful in calculations of flows with significant mean streamline curvature, flows with strong swirl or mean rotation, secondary flows in ducts, and flows with rapid variations in the mean flow. The Reynolds-stress models can be applied to any turbulent flow (Pope 2000). They provide the length, time and velocity scales information that are present in complex flow simulations. Consequently, they provide a suitable basis for the modeling of turbulent reactive flows, multiphase flows, etc. Such so-called second-moments closure has successfully been used in many complex turbulent flows. Since RSM accounts for the effects of streamline curvature, swirl, rotation, and rapid changes in strain rate in a more rigorous manner than the first-moment models, it has greater potential to give accurate predictions for complex flows. Beside these all benefits however they are substantially more complicated than the first-moment closure (such as κ−ε) and require much more coding efforts. Abandoning the isotropic eddy-viscosity hypothesis, the RSM closes the Reynolds-averaged Navier-Stokes equations by solving transport equations for the

Reynolds stresses together with another equations for the dissipation rate ($\varepsilon$) and turbulent kinetic energy (K). However, the fidelity of RSM predictions is still limited by the closure assumptions employed to model various terms in the exact transport equations for the Reynolds stresses. The modeling of the pressure-strain and the dissipation-rate terms is particularly challenging. But, the use of RSM is a must when flow features of interest are the result of anisotropy in the Reynolds stresses.

As a result of averaging the non-linear terms in the conservation equations, new unknown quantities appear in the averaged conservation equations, namely the six Reynolds stresses $\rho \overline{u_i u_j}$. Assuming a constant property flow:

$$\frac{\partial \overline{U_i}}{\partial x_i} = 0, \qquad (1)$$

$$\rho \overline{U_j} \frac{\partial \overline{U_i}}{\partial x_j} = -\frac{\partial p}{\partial x_i} + \frac{\partial}{\partial x_j}\left[\mu\left(\frac{\partial \overline{U_i}}{\partial x_j} + \frac{\partial \overline{U_j}}{\partial x_i}\right)\right] + \frac{\partial}{\partial x_j}(-\rho \overline{u_i u_j})$$

(2)

Equations (1) and (2) are called "Reynolds-averaged" Navier-Stokes (RANS) equations. They have the same general form as the instantaneous Navier-Stokes equations, with the variables now representing averaged values. Additional terms now appear that represent the effects of turbulent fluctuating. These "Reynolds stresses" terms must be modeled, in order to close equations. In the differential Reynolds stress models, transport equations are solved for individual Reynolds stress terms and for the dissipation rate, $\varepsilon$, (or for another quantity, e.g., $\omega$ which provides a length or time scale of the turbulence). The exact transport equations for these new unknown quantities may be written as:

$$\underbrace{\frac{\partial}{\partial t}\left(\rho \overline{u_i u_j}\right)}_{\text{Local Time Derivative}} + \underbrace{\frac{\partial}{\partial x_k}\left(\rho \overline{U_k}\,\overline{u_i u_j}\right)}_{C_{ij} = \text{Convection}} =$$

$$\underbrace{-\frac{\partial}{\partial x_k}\left[\rho \overline{u_i u_j u_k} + \overline{p(\delta_{kj} u_i + \delta_{ik} u_j)}\right]}_{D_{ij}^T = \text{Turbulent Diffusion}} + \underbrace{\frac{\partial}{\partial x_k}\left[\mu \frac{\partial}{\partial x_k}\left(\overline{u_i u_j}\right)\right]}_{D_{ij}^L = \text{Molecular Diffusion}}$$

$$\underbrace{-\rho\left(\overline{u_i u_k}\frac{\partial \overline{U_j}}{\partial x_k} + \overline{u_j u_k}\frac{\partial \overline{U_i}}{\partial x_k}\right)}_{P_{ij} = \text{Stress Production}} \qquad \underbrace{-\rho\beta\left(g_i \overline{u_j \theta} + g_j \overline{u_i \theta}\right)}_{G_{ij} = \text{Buoyancy Production}}$$

$$\underbrace{+ p\left(\frac{\partial u_i}{\partial x_j} + \frac{\partial u_j}{\partial x_i}\right)}_{\phi_{ij} = \text{Pressure Strain}} \qquad \underbrace{-2\mu \overline{\frac{\partial u_i}{\partial x_k}\frac{\partial u_j}{\partial x_k}}}_{\varepsilon_{ij} = \text{Dissipation}}$$

$$\underbrace{-2\rho\Omega_k\left(\overline{u_j u_m}\varepsilon_{ikm} + \overline{u_i u_m}\varepsilon_{jkm}\right)}_{F_{ij} = \text{Production by System Rotation}} \qquad (3)$$

3

Of the various terms in these exact equations, $C_{ij}$, $D_{ij}^L$, $P_{ij}$, and $F_{ij}$ do not require any modeling. However $D_{ij}^T$, $G_{ij}$, $\phi_{ij}$, and $\varepsilon_{ij}$ need to be modeled to close the equations. Many attempts by Rotta(1962), Launder and Shima(1989), Daly and Harlow (1970) Hanjalic and Launder(1972) Lumley and Khajeh-Nouri (1974) Launder et al.(1975) Chen and Rodi(1980), Fu et al.(1987), Speziale et al. (Pope 2000), etc. have been made to model the remaining terms to close the equation set. Recently, Pope(2000) has extensively considered this model in a graduate level text book named "Turbulent Flows". Also, Hwang and Jaw (1998) have reviewed some variations of second-moment closure turbulence models to show the capabilities and limitations of the existing turbulence models.

We need to derive models for the unknown components $D_{ij}^T$, $\phi_{ij}$, and $\varepsilon_{ij}$. With this modeling, many unknown components can be obtained in terms of original quantities $\overline{u_i u_j}$. Also, $k$, $\varepsilon$, and $\mu_t$ are obtained by SST model.

**Turbulent Diffusive Transport Model**
The simplest gradient-diffusion model for $D_{ij}^T$ due to Shir (Pope 2000) is:

$$D_{ij}^T = -\rho C_s \frac{k^2}{\varepsilon} \frac{\partial \overline{u_i u_j}}{\partial x_k}, \qquad (4)$$

Where, $C_s$ is a model constant. A more general use is the model of Daly and Harlow(1970) which uses the Reynolds-stress tensor to define an anisotropic diffusion coefficient:

$$D_{ij}^T = -C_s \rho \frac{k}{\varepsilon} \overline{u_k u_l} \frac{\partial}{\partial x_k}\left(\frac{\partial \overline{u_i u_j}}{\partial x_l}\right). \qquad (5)$$

However, this equation can result in numerical instabilities, so it has been simplified to use a scalar turbulent diffusivity as follows (Sarkar and Balakrishnan, 1990)

$$D_{ij}^T = \frac{\partial}{\partial x_k}\left(\frac{\mu_t}{\sigma_k}\frac{\partial \overline{u_i u_j}}{\partial x_k}\right) \qquad (6)$$

Where, $\mu_t$ is the eddy kinematic viscosity and the value of $\sigma_k$ is 1.0 in the standard and realizable k-$\varepsilon$ models. But, Lien and Leschziner (1994) derived a value of $\sigma_k$ = 0.82 by applying the generalized gradient-diffusion model, (Equation 6 to the case of a plane homogeneous shear flow).

**Pressure-Strain Model**
The pressure-strain term $\phi_{ij}$ in equation (3) is modeled according to the proposals by Gibson and Launder(1978), Fu et al.(1987) and Launder et al.(1975) The classical approach to modeling $\phi_{ij}$ uses the following decomposition:

$$\phi_{ij} = \phi_{ij,1} + \phi_{ij,2} + \phi_{ij,3}^\omega, \qquad (7)$$

where, $\phi_{ij,1}$ is the "slow pressure-strain" term,( also known as the "return-to-isotropy" term) and $\phi_{ij,2}$ is called the "rapid pressure-strain" term. The rapid term contains the mean velocity gradients, while the slow term contains only the fluctuating motion and $\phi_{ij,3}^\omega$ is the "wall-reflection" term.
The slow pressure-strain term ($\phi_{ij,1}$) is modeled as:

$$\phi_{ij,1} = -C_1 \rho \frac{\varepsilon}{k}\left[\overline{u_i u_j} - \frac{2}{3}\delta_{ij}k\right], \qquad (8)$$

where $C_1 = 1.8$.
The rapid pressure-strain term, $\phi_{ij,2}$, is modeled as:

$$\phi_{ij,2} = -C_2\left[\left(P_{ij} + F_{ij} + G_{ij} - C_{ij}\right) - \frac{2}{3}\delta_{ij}\left(P + G - C\right)\right], \quad (9)$$

where, $C_2 = 0.60$, $P_{ij}$, $F_{ij}$, $G_{ij}$ and $C_{ij}$ are defined as in equation (5), $P = \frac{1}{2}P_{kk}$, $G = \frac{1}{2}G_{kk}$, and $C = \frac{1}{2}C_{kk}$.

Here, $\phi_{ij,3}^\omega$ represents the pressure-strain wall-echo or wall-reflection term and is responsible for the redistribution of normal stresses near the wall. It tends to damp the normal stress perpendicular to the wall, while enhancing the stresses parallel to the wall. This term has been modeled by Launder and Shima (1989) as:

$$\phi_{ij,3}^\omega = C_1' \frac{\varepsilon}{k}\left(\overline{u_k u_m}\eta_k \eta_m \delta_{ij} - \frac{3}{2}\overline{u_i u_k}\eta_j \eta_k - \frac{3}{2}\overline{u_j u_k}\eta_i \eta_k\right)\frac{k^{3/2}}{C_\ell \varepsilon\, d}$$
$$+ C_2' \frac{\varepsilon}{k}\left(\phi_{km,2}\eta_k \eta_m \delta_{ij} - \frac{3}{2}\phi_{ik,2}\eta_j \eta_k - \frac{3}{2}\phi_{jk,2}\eta_i \eta_k\right)\frac{k^{3/2}}{C_\ell \varepsilon\, d},$$
$$(10)$$

where, $C_1' = 0.5$, $C_2' = 0.3$, $\eta_k$ is the $x_k$ component of the unit normal to the wall, $d$ is the normal distance to the wall, and $C_\ell = C_\mu^{3/4} / k$, where $C_\mu = 0.09$ and $k = 0.41$.

**Dissipation Tensor Model**
The dissipation tensor, $\varepsilon_{ij}$, is modeled as:

$$\varepsilon_{ij} = \frac{2}{3}\delta_{ij}\left(\rho\varepsilon + Y_M\right), \qquad (11)$$

where, $Y_M = 2\rho\varepsilon M_t^2$ is an additional "dilatation dissipation" term according to the model by Sarkar and Balakrishnan, (1990). The turbulent Mach number in this term is defined as:

$$M_t = \left(k / a^2\right)^{1/2}, \qquad (12)$$

Where, $a = \left(\gamma R T\right)^{1/2}$ is the speed of sound. Equation (11) for incompressible flows or low Mach number flows reduces to

$$\varepsilon_{ij} = \frac{2}{3}\delta_{ij}\left(\rho\varepsilon\right),$$ that is similar to Hanjalic and Launder(1972) model.

**SST TURBULENCE MODEL**
The SST turbulence model uses the ($\kappa - \omega$) model in the sub layer as well as in the logarithmic part of the boundary layer. In the wake region of the boundary layer, the ($\kappa - \omega$) model has to be abandoned in favor of the ($\kappa - \varepsilon$) model. The reason for this switch is that the ($\kappa - \omega$) model has a very strong sensitivity to the free stream values of $\omega$, but the ($\kappa - \varepsilon$) model does not suffer from this deficiency. The equations of the SST model are:

$$\frac{D\rho k}{Dt} = \tau_{ij}\frac{\partial \overline{U_i}}{\partial x_j} - \beta^* \rho\omega k + \frac{\partial}{\partial x_j}\left[\left(\mu + \sigma_k \mu_t\right)\frac{\partial k}{\partial x_j}\right]$$
$$(7)$$

$$\frac{D\rho\omega}{Dt} = \frac{\gamma}{\nu_t}\tau_{ij}\frac{\partial \overline{U_i}}{\partial x_j} - \beta\rho\omega^2 + \frac{\partial}{\partial x_j}\left[\left(\mu + \sigma_\omega \mu_t\right)\frac{\partial \omega}{\partial x_j}\right]$$
$$+ 2\rho(1 - F1)\sigma_{\omega 2}\frac{1}{\omega}\frac{\partial k}{\partial x_j}\frac{\partial \omega}{\partial x_j}, \qquad (13)$$

Where, $\omega$ is the specific dissipation rate $\left(\varepsilon / \beta^* k\right)$, $\tau_{ij}$ are the

Reynolds stresses, and the left hand sides of the equations are the Lagrangian derivative ($D/Dt = \partial/\partial t + u_i \partial/\partial x_i$). The eddy kinematics viscosity, $\nu_t$, is:

$$\nu_t = \frac{a_1 k}{\max(a_1 \omega, SF_2)}, \tag{14}$$

$$S = \left[ \left( \frac{\partial \overline{U_i}}{\partial x_j} + \frac{\partial \overline{U_j}}{\partial x_i} \right) \frac{\partial \overline{U_i}}{\partial x_j} \right]^{1/2}. \tag{15}$$

The switching function $F_1$ is such that, it is unity near the surface and is zero away from it, resulting in the ($\kappa-\omega$) model in the near-wall region and the ($\kappa-\varepsilon$) model in the remainder of the flow-field. The values of the constants $\sigma_k$, $\sigma_\omega$, $\sigma_{\omega 2}$, $\beta$, $\beta^*$, $\gamma$, and relations defining the switching function: $F_1, F_2$, $a_1$ are given by Menter (1992, 1994).

## COMPUTATIONAL METHODOLOGIES

A FORTRAN computer program is obtained to solve the incompressible, turbulent, time averaged, and three-dimensional Navier-Stokes equations (RANS) using Reynodls stress turbulence model (RSM) for the closure problem. In this work, a finite-volume, hybrid, SIMPLE method with a non-uniform staggered grid is used, in which the vector components are stored in the control volume faces and the scalar quantities are stored inside the control volume. The grid is cluster near the jets exit in (x, y) plane and near the wall in y direction. A line-by-line algorithm is used to solve the discretized algebraic equations (tri-diagonal coefficient matrix) with appropriate under-relaxation factor for faster convergence.

## COMPUTATIONAL AND PHYSICAL DOMAINS

**Past approach (Ordinary film cooling scheme):** Figure 1 shows the past approach film cooling in our previous work (Javadi et. al. 2002). This computational domain defines a row of rectangular jets which are injected at $90^\circ$ to the cross flow (main stream flow). Considering a periodic boundary condition imposed in the spanwise direction (with a distance equal to 3D) our computational domain is condensed to a single jet study and the main flow above it. The square jets diameter is D. The geometry of the problem has been non-dimensionalized by D. The origin of the coordinate system used is located at the center of the jet exit. The jet channel's length is $5D$ and the cross-flow region is extended from $5D$ upstream of the center of the jet to $40D$ downstream. In the vertical direction, the domain extends $20D$ above the flat plate. Flow-field characteristics of jets in a cross-flow are strongly dependent on the momentum ratio. Here, the main stream and the jet fluids were considered both to be air and therefore the momentum ratio "$J$" is replaced by velocity ratio "R".

Two cases of $R$ (0.5, 1.5) were considered in this study. For these cases, the jet velocity at the inlet of the channel was maintained at 5.5 m/s; therefore, the cross-flow velocities used were 3.67, and 11.0 m/s. Also, the jet diameter $D$ was 12.7 mm. throughout this paper, references are made to the "diameter" of the jet. This terminology is rooted in the past study of jets, where round jets are customarily used. Thus, the term "diameter" is equivalent to the "jet width." Based on this length scale, a jet Reynolds number, defined as $\mathrm{Re}_{jet} = \rho V_{jet} D / \mu$ was obtained to be 4700, which was kept constant throughout this study.
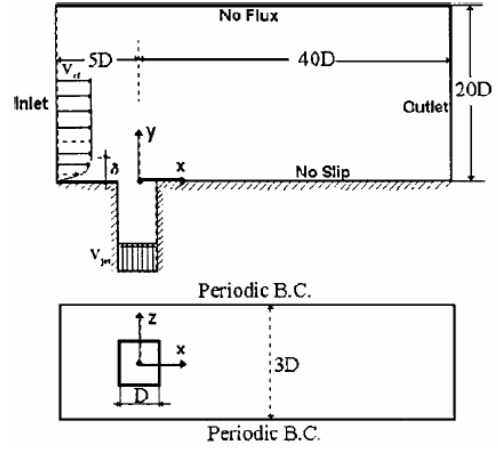


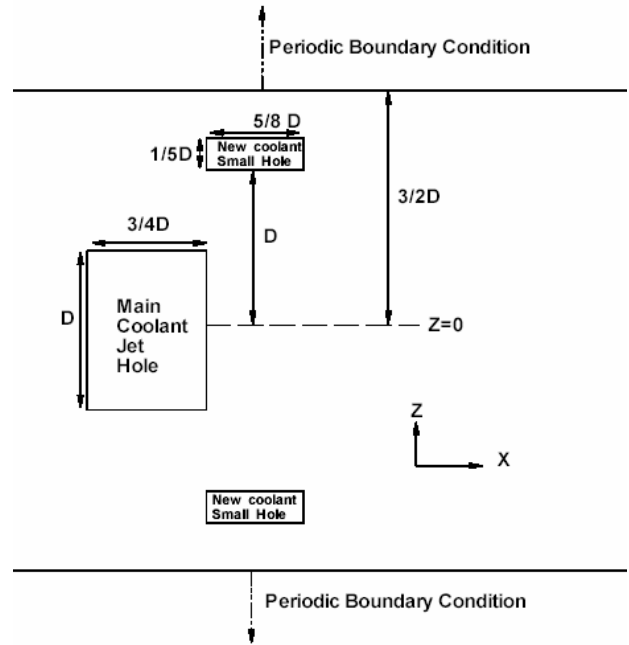**Fig.1:** Ordinary film cooling,



**Fig. 2**: Our new film cooling scheme show new coolant small jets holes beside the main coolant jet hole

**New film cooling scheme (combined jets idea):**

Figure 2 shows the schematic of our new system in this paper. we have considered a new combined jets system including main coolant jet and two additional coolant small jets (coupled), downstream of the main jet in order to control the interaction and mixing between two hot and cold streams. Note, in order for the results to be comparable, total coolant air and the cross section area of the new combined jets system are the same as the previously used single jet (ordinary system). In the other word the summation of coolant rate and cross section of two new coolant small jets hole ($5/8D \times 1/5D$) and the new main coolant jet hole ($D \times 3/4D$) in our combined system is equal to previous hole ($D \times D$) in ordinary film cooling. Other parameters such as main cross flow properties, temperature and total coolant mass flow rate, the jet channel's length (equal to $5D$) the cross-flow region (from $5D$ upstream of the center of the jet to $40D$ downstream), and etc

are the same as to our previous system. It is clear that some parameter such as Reynolds number may be change relative to ordinary system that can be discuss. However, the most effect of these new small jets is reducing of interaction and mixing process by generation new weak wakes that is discussed here.

**Boundary Conditions**

In this work, we used five types of boundary conditions, namely, inlet, outlet, no-flux, periodic and wall. Each of these boundary conditions are briefly discussed below:

**1.** Inlet Boundary Condition: At the inlet, the boundary layer thickness is set to 2D to match the experimental data. For the boundary layer at the inlet plane of the main flow, the 1/7th power-law profile is used for u-velocity component and a uniform velocity is imposed above y=2D, and other velocity components are set to zero. The value of turbulent kinetic energy is calculated from Ajersch et al. (1995) experimental data.

For R=1.5 , the value of turbulent kinetic energy is approximated to be 2% of $V_{cf}$. For R=0.5, this value is approximated to be 1.2% of $V_{cf}$. The value of the Reynolds stress terms are calculated from $\overline{u'_i u'_j}$=a×k (i, j=1, 2, 3). Since turbulence is non-isotropic, the value of a=1/3 for i=j=1, a=1/6 for i=j=2, 3, and zero for i≠j. The inlet turbulence energy dissipation rate can be obtained from below formula:

$$\varepsilon_{in} = C_\mu^{\frac{3}{4}}(k^{\frac{3}{2}}/L_m), \qquad (11\text{-}a)$$

$$\omega_{in} = \frac{(1 \rightarrow 10)V_{cf}}{L}, \qquad (11\text{-}b)$$

Where, $C_\mu$ is an experimental constant and is equal to 0.09, $L_m$ is the Prandtl's mixing length scale, and L is the approximate length of the computational domain.

**2.** Outlet Boundary Condition: At the outlet, we used zero gradients, since there is no guarantee for conservation of mass during SIMPLE iteration, we used the below relation for velocity component.

$$\overline{u}_{NI,J,K} = \overline{u}_{NI-1,J,K}(\dot{M}_{in}/\dot{M}_{out}) \qquad (23)$$

Where, $\dot{M}_{in}$ and $\dot{M}_{out}$ are the inlet and outlet mass flow, respectively.

**3.** No Flux Boundary Condition: We set V=0.0 at this boundary and for other dependent variables we used the below relation:

$$\frac{\partial \phi}{\partial n} = 0.0, \qquad (24)$$

where, $\phi$ is any dependent variable (except V) and $n$ is the normal vector of the face.

**4.** Periodic Boundary Condition: Periodic boundary condition is imposed in the spanwise direction. At this boundary, for all dependent variables we used the below relation:

$$\phi_{i,j,1} = \phi_{i,j,NK-1}; \phi_{i,j,NK} = \phi_{i,j,2}. \qquad (25)$$

But, since we used a staggered grid in our study, the periodic condition for w component is:

$$w_{i,j,2} = w_{i,j,NK-1} , \ w_{i,j,NK} = w_{i,j,3} , \qquad (26)$$

**5.** Solid-Wall: In this study, we assumed that the wall is adiabatic and has no-slip. For the SST model, the turbulence kinetic energy was set to zero at the walls and $\omega$ was obtained by the following relation suggested by Menter (1994):

$$\omega = 60\upsilon / \beta_1(\Delta y_1)^2 \qquad (27)$$

where, $\Delta y_1$ is the distance to the next point away from the wall, $\upsilon$ is the molecular kinematics viscosity, and $\beta_1$ is a constant. Also, using a local coordinate system, where $\tau$ is the tangential coordinate, $\eta$ is the normal coordinate, and $\lambda$ is the binormal coordinate, the Reynolds stresses at the wall-adjacent cells are computed from (Pope, 2000, and Menter, 1994) as :

$$\frac{u'^2_\tau}{k} = 1.098 \ , \qquad \frac{u'^2_\eta}{k} = 0.247,$$

$$\frac{u'^2_\lambda}{k} = 0.665 \ , \qquad \frac{u'_\tau \, u'_\eta}{k} = -0.255 . \qquad (28)$$

The same boundary conditions were used for the jet channel walls.

## RESULTS AND DISCUSSION

We computationally solve the three-dimensional turbulent flow using the SIMPLE finite volume method implemented with RSM/SST turbulence model. Code validation and grid resolution study has been shown for ordinary film cooling scheme in our previous work (Javadi et. al 2002). In this regard the results of our code compared with the experimental data of Ajersch et al (1995) experimental data in which the flow of a row of six square jets injected at 90 degrees to a cross flow, both experimentally (using a three-component Laser Doppler velocimeter) and computationally have been studied. Additionally our results were compared with Keimasi and Taeibi-Rahani's numerical simulation (2001). The comparison between the measured data and numerical solution results showed that RSM/SST turbulence model in our work performed better agreement with experimental data in most cases. Figures 3 and 4 show the comparison our computational results with the experimental data and other computational results for prediction of streamwise and vertical velocities when R=0.5, Z/D=0.0 and X/D =0. Although there is good agreement between both various computational works and experimental data in figure 3, however in Fig. 4 our numerical solution with RSM/SST turbulence modeling performs better agreement with the experimental data. Similarly figures 5 and 6 show that our computational code suitably predicts the high sensitive variables such as shear stress terms and turbulence kinetic energy. This is a strong indication of high capability of our numerical scheme for predicting such sensitive variables (Javadi et. al, 2002).

After the code validation, the new combined jets (or Coupled jets) mechanism and its results to enhance film cooling effectiveness are discussed. Figure 7 shows the complexity of a 3D flow filed in an ordinary film cooling approach. Figure 8 shows the result of this type of film cooling. The figure shows the temperature distribution close to the wall. We see no good cooling effectiveness and uniformity over the plate. In the other hand figure 9 similarly shows the distribution of temperature using the combined jets idea innovated in our work. this figure show a significant enhancement in film cooling effectiveness in addition to a good improvement in uniformity of the coolant film on the plate It should be emphasized again, in order for the results to be comparable, total coolant air and the cross section area of the new combined jets system are the same as the previously used single jet (ordinary system).

For better understanding of the mechanism of this improvement, the role of the new weak wakes generated by the coupled jets beside the strong main wakes generated by main jet is discussed. Fig. 10 shows a high interaction between a strong coolant wake and hot cross flow in ordinary film cooling.
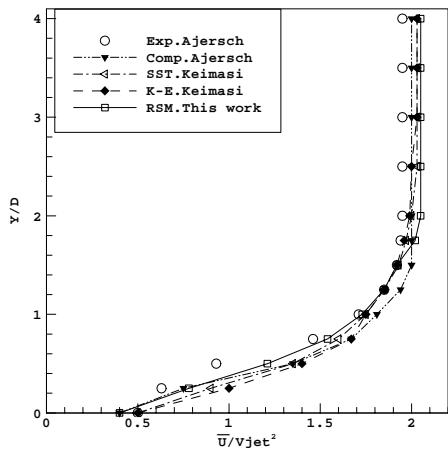
**Fig. 3:** Comparison of mean streamwise velocity at jet center plane (*z/D* = 0) for X/D= 0 and *R* = 0.5
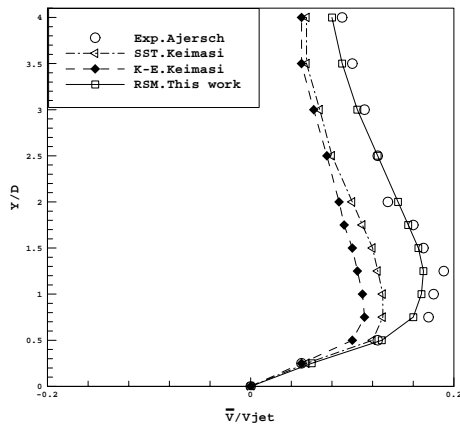


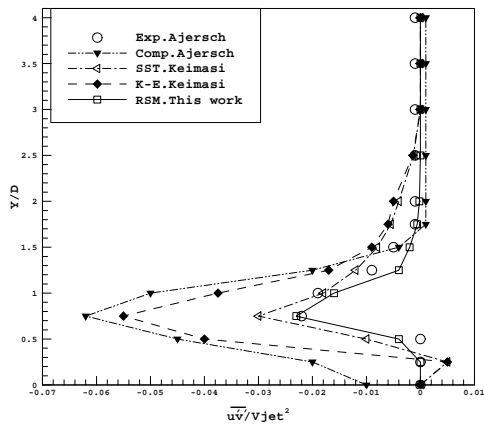**Fig. 4:** Comparison of vertical velocity at *z/D* = - 1 for X/D=0 *and R* = 0.5.



**Fig. 5:** Comparison of shear stress ($\overline{uv}/V_{jet}^2$) at jet center plane for x/D=3 and R = 0.5 and
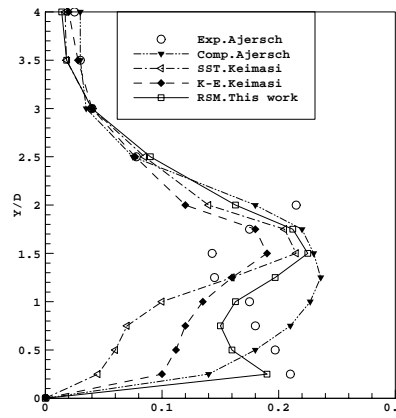


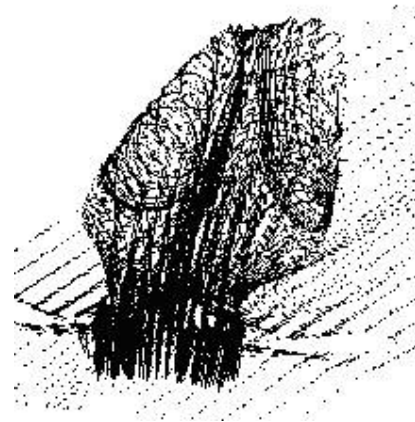**Fig. 6:** Comparison of turbulence kinetic energy at jet center plane for X/D=3 and *R*= 1.5



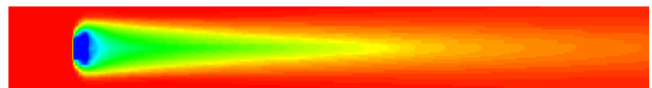**Fig. 7:** complexity of a 3D flow filed in ordinary film cooling scheme.



**Fig. 8:** No good cooling effectiveness and uniformity over the plate in ordinary film cooling, Deg=90, R=0.5,
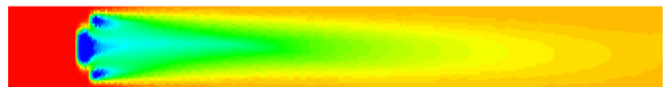


**Fig. 9:** Combined jet scheme shows a high effectiveness and good cooling uniformity over the plate, Deg=90, R=0.5, with a same coolant air and total cross section of coolant hole in both system



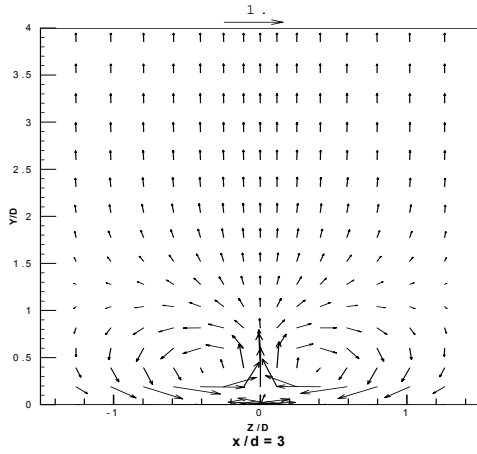T: 313.385  409.511  505.637  601.764  697.890  794.016  890.142  986.268
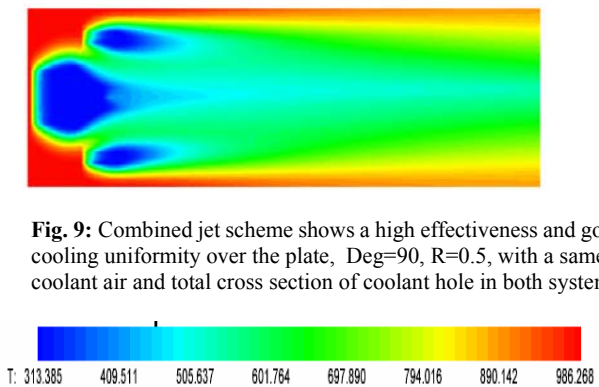
**Fig 10:** The high interaction between a strong coolant wake and hot cross flow in ordinary film cooling
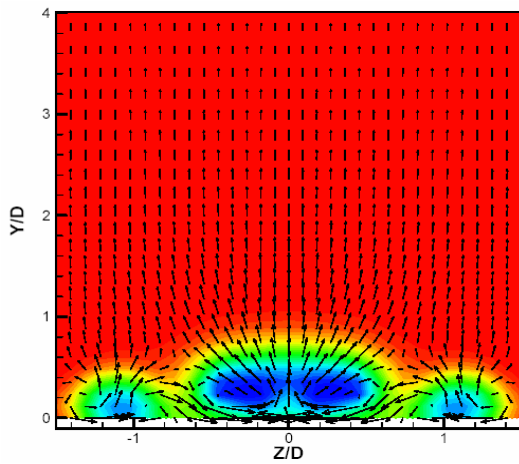


**Fig 11:** New weak wakes generated by small coolant hole such as a fluid barrier reduce the interaction and mixing process of the hot and main cooled stream
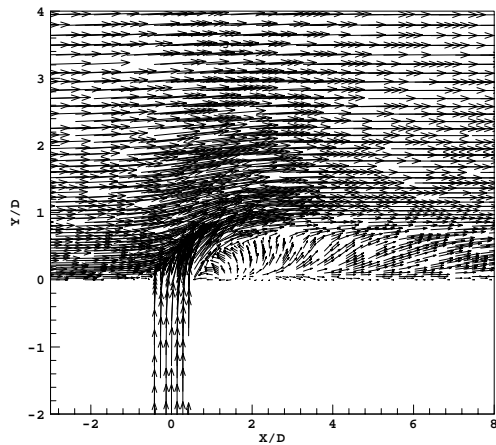


**Fig. 12:** Velocity vectors at jet center plane (*z/D*=0) for the velocity ratio of 0.5. Shows high interaction mixing zone simultaneously remarkable vortex at X/D between 0.5 and 5 for a jet-to-crossflow in ordinary system
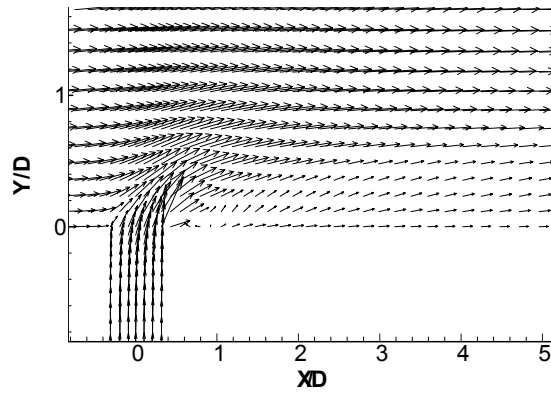


**Fig. 13:** Velocity vectors at jet center plane (*z/D*=0) for the velocity ratio of 0.5 in our combined jets scheme shows the arrival of a coolant jet without remarkable vortex at X/D between 0.5 and 5. It seems a weak interaction and mixing in this because of the effects of small coolant jets that are in another z/D plane (started at z/D=$\pm 1$ ) and it can't be seen them here
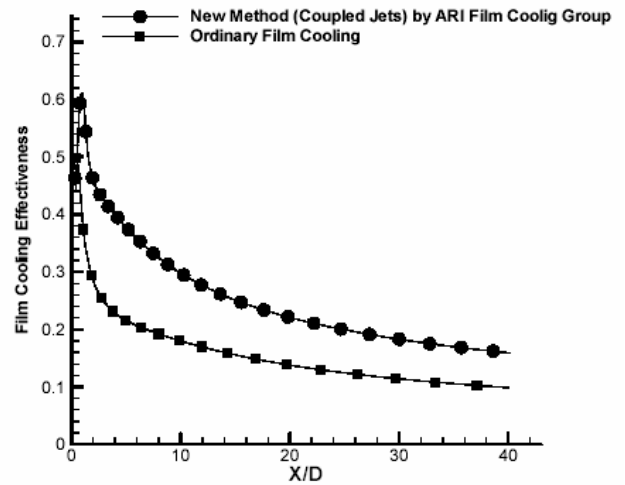


**Fig.14:** A drastic improvement in film cooling effectiveness for our new combined jet system (Coupled Jets film cooling) with same total coolant rate and cross section coolant hole relative to ordinary system Deg=90, R=0.5,

While in Fig. 11 we see a weak interaction and mixing process between two hot crossflow and main cooled streams because of the action of the new weak wakes generated by small coolant holes. These new weak wakes reduce the interaction and mixing process the hot and main cooled stream like a fluid barrier while they do not have themselves high interactions with hot stream. On the other hand it seems that not only the interaction between the new weak wakes and the main strong wakes isn't undesirable, but also it is useful for accomplishing a desirable momentum and energy transport in spanwise direction and achieves a uniform coolant film. Hence, the improvement of the cooling uniformity is another benefit of this new scheme, which will be the subject of our future work.

Figures 12 and 13 demonstrate the velocity field for both past and new approach. Figure 12 shows a high interaction between hot at 0.5< *X/D* <5 if an ordinary film cooling jet-to-cross flow

approach used. However figure 13 shows the arrival of a coolant jet without introducing high vorticity in the wake zone. An evidently weak interaction and dilute mixing is seen in this figure. It is because of the effects of small coolant jets that are in another z/D plane (started at z/D=$\pm 1$ ) which can not be seen here. However they can be seen in figure 11. Finally, Fig. 14 shows a drastic improvement in film cooling effectiveness (more than 50%) for using new approach combined jet system (Coupled Jets film cooling) in our research. As was told, it should be emphasized again that total coolant air and the cross section area of the new combined jets system are the same as the previously used single jet (ordinary system). More investigation for evaluation of capability of suction stream instead of blowing in the small coupled jets, and parametric study of the effects of the hole shape, jet angle, blowing ratio, jets array, and coolant temperature effects in this new scheme will be the subject of our future work.

**Conclusion**
We developed a new approach to achieve a high film cooling effectiveness and uniformity  by the control the wake zones behind the coolant jet and reduction of mixing strength, between the two hot (main Stream) and cold streams (coolant jets), using combined jets. For this purpose we considered a new combined jets system including main coolant jet and two additional coolant small jets (coupled), downstream of the main jet in order to control the interaction and mixing between two hot and cold streams.  The results shows a drastic improvement in film cooling effectiveness (more than 50%) for using new approach combined jet system (Coupled Jets film cooling) in our research. It should be emphasized that total mass coolant air and the cross section area of the new combined jets system were the same as the previously used single jet (ordinary system).  Our numerical simulation results of this new approach demonstrate that the new weak wakes generated by the small coupled jets beside the strong main wakes generated by main jet have principal role in this improvement.
These new weak wakes reduce the interaction and mixing process the hot and main cooled stream like a fluid barrier while they do not have themselves high interactions with hot stream. On the other hand it seems that not only the interaction between the new weak wakes and the main strong wakes isn't undesirable, but also it is useful for accomplishing a desirable momentum and energy transport in spanwise direction and achieves a uniform coolant film. Hence, the improvement of the cooling uniformity is another benefit of this new approach.

# Reference

Ajersch, P., Zhou, J. M., Ketler, S., Salcudean, M., and Gartshore, I. S., "Multiple Jets in a Crossflow: Detailed Measurements and Numerical Simulations," International Gas Turbine and Aeroengine Congress and Exposition. ASME Paper 95-GT-9, Houston, TX, June 1995, pp. 1–16.

Amer, A. A., Jubran, B. A., and Hamdan, M. A., 1992,  "Comparison of Different Two-Equation Turbulence Models for Prediction of Film Cooling from Two Rows of Holes," Numerical Heat Transfer, Pt. A, Vol. 21, pp. 143–162.

Chen, C. J. and Rodi W. (1980), "Vertical Turbulent Buoyant jets -A Review of Experimental Data", The Science and Application of Heat and Mass Transfer Series, HMT, Vol. 4. Pergamon, NY, U.S.A.

Daly, B.J. and Harlow, F.H., 1970. "Transport Equations of Turbulence," Physics Fluids, Vol. B, pp. 2634–2649.

Eckert E.R.G, and  Livin good, J.N.B 1954, " Comparsian of Effectiveness of Convection, Transpiration, an Film-Cooling Methods With Air as Coolant" , NASA-Report-1182.

Fu S., Launder B. E. and Leschziner M. A., 1987, "Modeling St rongly Swirling Recirculating Jet Flow with Reynolds-Stress Transport Closures. Sixth Symposium on Turbulent Shear Flows, Toulouse, France.

Gibson M. M. and Launder B. E., 1978, "Ground Effects on Pressure Fluctuations in the Atmospheric Boundary Layer", J. Fluid Mech., 86, pp.491—511.

Hanjalic, K. and B. E. Launder, 1972, " A Reynolds Stress Model of Turbulence and its Application to Thin Shear". J. Fluid Mechanics, 52(4), pp. 609-638.

Hassan, I., Findlay, M., Salcudean,M., and Gartshore, I., 1998, "Prediction of Film Cooling with Compound-Angle Injection Using Different Turbulence Models," 6th Annual Conf. of the Computational Fluid Dynamics Society of Canada, Quebec, QC, Canada, pp. 1–6.

Hwang R.R. and Jaw S.Y. 1998, " Second-Order Closure Turbulence Models: Their Achievements and Limitations" Proc. Natl. Sci. Counc. ROC (A) Vol. 22, No. 6, pp. 703-722

Javadi A., Javadi K., Taeibi-Rahni M. and Keimasi M., 2002, "Reynolds stress turbulence models for prediction of shear stress terms in cross flow film cooling – numerical simulation", 4th International ASME/JSME/KSME Symposium on computational technology CFD) for fluid/thermal/chemical/stress systems and industrial application  August, 2002, Hyatt Regency, Vancouver, CANADA.

Keimasi, M.R., and Taeibi-Rahni M., 2001, "Numerical Simulation of Jets in a Crossflow Using Different Turbulence Models", AIAA JOURNAL, Vol. 39, No. 12, pp. 2268- 2277

Kim, S. W. and Benson, T.J., 1993, "Fluid Flow of a Row of Jets in Cross flow-A Numerical Study", AIAA J., Vol. 31,No. 5, pp. 806-811.

Launder B. E., Reece G. J., and Rodi. W., 1975, " Progress in the Development of a Reynolds-Stress Turbulence Closure", J. Fluid Mech., 68 (3), pp. 537-566.

Launder B. E. and Shima N., 1989, "Second-Moment Closure for the Near-Wall Sub Layer: Development and Application" AIAA J., 27(10), pp.1319-1325.

Lien F. S., Leschziner M. A. 1994, "Assessment of Turbulent Transport Models Including Non-Linear RNG Eddy-Viscosity Formulation and Second Moment Closure" Computers and Fluids, 23(8), pp.983-1004.

Lumley J. L. and Khajeh-Nouri B. J., 1974, "Computational Modeling of Turbulent Transport". Adv. Geophys., 18A, pp. 169-92.

Medic G. and Durbin P., 2001, " Numerical Simulation of Heat Transfer Around Film-Cooled Gas Turbine Blades", Submitted to J. Turbomachinary.

Menter, F. R., 1994, "Two-Equation Eddy-Viscosity Turbulence Models for Engineering Applications," AIAA J., Vol. 32, No. 8, pp. 1598–1605.

Menter, F. R., 1992, "Performance of Popular Turbulence Models for Attached and Separated Adverse Pressure Gradient Flows," AIAA J., Vol. 30, No. 8, pp. 2066–2072.

Pope. "Turbulent Flows", 2000, Cambridge University.

Rotta, J. 1962, "Turbulent Boundary Layers in Incompressible Flow", Progress in Aero. Sci., Vol. 2.

Sarkar S. and Balakrishnan L., 1990, "Application of a Reynolds-Stress Turbulence Model to the Compressible Shear Layer".  ICASE Report 90-18, NASA CR 182002.